ORIGINAL RESEARCH PAPER
Volume - 14 | Issue - 08 | August - 2025 | PRINT ISSN No. 2277 - 8179 | DOI : 10.36106/ijsr
INTERNATIONAL JOURNAL OF SCIENTIFIC RESEARCH

SIGNIFICANT PROPERTIES OF OPTICAL AND SURFACE MORPHOLOGY FOR METALLIC AND NON METALLIC ROCKS MINERALS EXISTING IN AREA OF KUTCH, GUJARAT

Earth Science

Juhiben P Patel Research Scholar
Dr. Kishor Patel Assi. Prof

ABSTRACT

Spectroscopic techniques play a crucial role in mineral characterization, offering detailed insights into the physical, chemical, and structural attributes of diverse mineral systems. This study focuses on the analysis of Bentonite, Bauxite, Gypsum, and Sandstone samples from Kutch, Gujarat, employing a range of modern spectroscopic methods including Fourier Transform Infrared (FT-IR) Spectroscopy, X-ray Diffraction (XRD), and X-ray Fluorescence (XRF). These techniques allow precise identification of functional groups, crystalline phases, and compositional variations, which are essential for assessing their industrial utility and geological significance. The results highlight characteristic spectral features, such as hydroxyl and silicate bands in Bentonite, aluminum hydroxide and carbonate signatures in Bauxite, sulfate and water-related vibrations in Gypsum, and dominant silicate features in Sandstone. The integration of these spectroscopic methods not only confirms mineralogical compositions but also provides insights into phase transitions, impurity content, and structural frameworks. Additionally, combining spectroscopic data with computational interpretation enhances the understanding of complex interactions within these mineral systems. This investigation demonstrates the value of advanced spectroscopic approaches in exploring the mineral wealth of Kutch, supporting their applications in industries like ceramics, cement, refractories, and construction materials, while contributing to broader geological research.

KEYWORDS

Metallic and Non Metallic Minerals, Bentonite, Bauxite, Gypsum, Sand Stone

INTRODUCTION

This study investigates the structural, optical, and spectroscopic properties of four key metallic and non-metallic minerals—Bentonite, Bauxite, Gypsum, and Sandstone—collected from the Kutch region of Gujarat[1]. The optical behavior of these minerals is largely governed by their refractive index and extinction coefficients, which define their interaction with incident radiation in terms of absorption, reflection, and emission. Variations in energy states within the mineral matrix lead to characteristic absorption and emission patterns, with hydrated and hydroxyl-bearing phases, such as those in Bentonite and Gypsum, displaying pronounced vibrational features in the mid-infrared region, particularly near 10 and 20 µm due to silicate and sulfate resonances. Ultraviolet-visible (UV-Vis) spectroscopy (190–900 nm)[2] further elucidates the electronic and optical properties of these minerals. The linear relationship between absorbance and concentration allows for reliable quantitative assessment, while the excitation of electrons by UV-Vis photons highlights band gap transitions, impurity levels, and trace elements[3]. Silicate-rich Bentonite and Sandstone exhibit distinct electronic transitions, whereas Bauxite and Gypsum reveal features associated with aluminum hydroxides and sulfate units[4], respectively, aiding in their industrial and technological evaluation. Infrared (IR) spectroscopy complements these findings by identifying vibrational modes of complex anions (SO_4^{2-}, PO_4^{3-}, SiO_4^{4-}) and water-related groups, along with lattice vibrations from structural frameworks. FT-IR and FT-Raman spectra confirm the dominant structural units: Si–O stretches and bends in Bentonite and Sandstone, SO_4^{2-} modes in Gypsum, and Al–O–H features in Bauxite[5]. X-ray diffraction analysis validates their crystalline phases, revealing layered aluminosilicates, Boehmite/gibbsite structures, monoclinic Gypsum, and quartz-rich Sandstone. Collectively, these spectroscopic and diffraction studies provide a comprehensive understanding of the structural, chemical, and optical characteristics of Kutch's mineral resources, highlighting their compositional integrity and potential for industrial, environmental, and technological applications[6].

Bentonite, Bauxite, Gypsum, and Sandstone represent some of the most significant metallic and non-metallic mineral resources in the Kutch region of Gujarat, India, contributing extensively to industrial, construction, and environmental applications. These minerals, owing to their unique structural and chemical compositions, exhibit diverse optical and spectroscopic behaviors, making them valuable for both geological characterization and industrial utilization. India hosts abundant reserves of such minerals, with Kutch recognized as a prominent hub for aluminosilicates (Bentonite and Bauxite), hydrated sulfates (Gypsum), and silicate-rich sedimentary rocks (Sandstone), which collectively form a substantial base for regional economic and industrial growth[7].

The structural complexity of these minerals arises from their varied crystalline frameworks: Bentonite, a layered aluminosilicate clay, features expandable smectite sheets with interlayer water and exchangeable cations; Bauxite primarily comprises aluminum hydroxides such as gibbsite and boehmite; Gypsum ($CaSO_4 \cdot 2H_2O$) consists of a monoclinic crystal lattice with coordinated water molecules; while Sandstone is dominated by quartz (SiO_2) with minor feldspar and clay components. Impurities, including trace metals (e.g., Fe, Mg) and hydroxyl groups, further influence their spectroscopic signatures and thermal stability[8].

High-resolution spectroscopic techniques such as FT-IR, FT-Raman, UV-Vis, and solid-state Nuclear Magnetic Resonance (NMR) spectroscopy, combined with X-ray diffraction (XRD), are essential for elucidating the structural, electronic, and vibrational properties of these minerals. Magic Angle Spinning (MAS) NMR, in particular, is a powerful approach for resolving isotropic chemical shifts of nuclei such as ^{27}Al, ^{29}Si, and, where applicable, ^{13}C, enabling insights into their local bonding environments and structural order[9]. These methods collectively allow the identification of key vibrational modes (e.g., Si–O, Al–O, SO_4^{2-}), assessment of hydration states, detection of isomorphic substitutions, and determination of crystallinity, all of which are crucial for evaluating the quality and industrial suitability of these mineral deposits[10].

The present study focuses on systematically characterizing the structural, vibrational, and electronic properties of Bentonite, Bauxite, Gypsum, and Sandstone from Kutch, using a combination of advanced spectroscopic and diffraction techniques, with the objective of correlating their mineralogical features to potential industrial applications[11].

MATERIALS AND METHODS

Representative samples of Bentonite, Bauxite, Gypsum, and Sandstone from the Kutch region were ground to fine powders using an agate mortar and pestle to prevent contamination. The powdered materials were sieved, and particles smaller than 50 µm were collected for analysis. These samples were subjected to X-ray diffraction (XRD), Fourier-transform infrared spectroscopy (FT-IR), Fourier-transform Raman (FT-Raman), and solid-state nuclear magnetic resonance (NMR) spectroscopy to investigate their structural and spectroscopic properties[12]. X-ray diffraction (XRD) patterns were recorded using a SEIFERT X-ray diffractometer equipped with Cu Kα radiation (λ = 1.54 Å), a copper filter on the secondary optics, operating at 45 kV and 20 mA. Powdered samples were mounted on quartz supports to minimize background interference[13]. FT-IR spectra were obtained using a PerkinElmer Spectrum One spectrometer, with the samples prepared in KBr pellets. Spectra were collected in the 4000–400 cm^{-1} range, and the band intensities were expressed as transmittance (%)[15]. FT-Raman spectra were recorded using a

Bruker IFS system with an FRA Raman attachment, employing an Nd:YAG laser source (1064 nm). Spectra were traced in the 3500–50 cm^{-1} region, averaging 500 scans at a resolution of 0.1 cm^{-1}. These analyses allowed identification of the fundamental molecular vibrations, including silicate, hydroxyl, and sulfate groups, characteristic of the studied minerals[14]. The X-band EPR spectra of Bentonite, Bauxite, Gypsum, and Sandstone samples were recorded using a JEOL JES-TE100 EPR spectrometer. The measurements were carried out with a field modulation frequency of 100 kHz and a microwave power of 1 mW to ensure optimal signal resolution while minimizing sample heating. 1,1-Diphenyl-2-picrylhydrazyl (DPPH) was used as an external field marker for accurate g-factor calibration. The spectra provided valuable information on the presence of paramagnetic species, such as transition metal ions (Fe^{3+}, Mn^{2+}) and defects within the mineral lattices, which contribute to their electronic and magnetic properties[16].

RESULTS AND DISCUSSION

1. FT-IR Spectroscopy

The FT-IR spectra of Bentonite, Bauxite, Gypsum, and Sandstone from Kutch, Gujarat, reveal distinct vibrational features corresponding to their major mineral phases (Table 1). Bentonite shows strong OH-stretching at 3695–3622 cm^{-1} (structural hydroxyl) and a broad water band near 3425 cm^{-1}. Intense Si–O stretching at 1109–1035 cm^{-1} and Al–OH bending at 912 cm^{-1} confirm smectite dominance. Bauxite displays a broad OH band near 3429 cm^{-1}, Al–O stretching at 1043 cm^{-1}, and deformation bands at 550 and 461 cm^{-1}, typical of gibbsite and boehmite[18]. Weak carbonate-associated features appear at 1631 and 1440 cm^{-1}. Sandstone exhibits strong quartz Si–O stretching at 1063 cm^{-1}, bending at 464–683 cm^{-1}, and overtones near 799 cm^{-1}, with a minor water band at 3440 cm^{-1}. Gypsum is characterized by sulfate vibrations: asymmetric stretching at 1076 cm^{-1}, bending at 710 and 460 cm^{-1}, and water-related bands at 3441 and 1620 cm^{-1}. Carbonate overtones near 1425 cm^{-1} and combination bands (1800–2515 cm^{-1}) reflect its hydrated structure. These spectral signatures confirm the primary mineralogy and provide structural insights into the industrially important Kutch deposits[17-20].

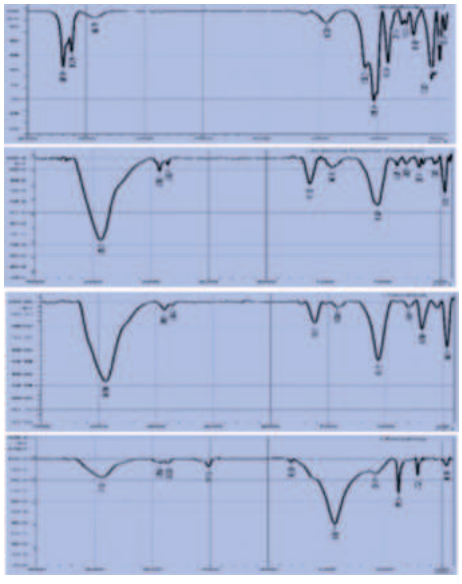

Figure 1: FT-IR Spectra for Metallic and Non Metallic Minerals.

Vibrational Assignments and Interpretation of Spectroscopic Features

The FTIR spectra of Bauxite, Gypsum, Bentonite, and Sandstone were analyzed to identify characteristic vibrational modes associated with their functional groups and structural units (Figs. 1). The observed peak positions and their corresponding assignments are summarized in Table 1. Band assignments were carried out based on comparison with previously reported experimental data and literature values for aluminosilicates, carbonates, sulfates, and silicates (Farmer, 1974; Madejová, 2003; Sipos et al., 2008).

For all four minerals, the broad absorption bands near 3400–3600 cm^{-1} are attributed to O–H stretching vibrations, arising from structural hydroxyl groups or adsorbed water. In Bauxite, distinct peaks at ~3695 and 3622 cm^{-1} confirm the presence of gibbsite and kaolinite phases. Gypsum displays sharp sulfate-related features, including symmetric and asymmetric SO_4^{2-} stretches around 1100–1000 cm^{-1}. Bentonite shows strong Si–O stretching at ~1060 cm^{-1}, along with characteristic Al–OH bending modes. Sandstone exhibits dominant silicate peaks[22], including Si–O–Si asymmetric stretches (~1070–1020 cm^{-1}) and lattice vibrations near 470–460 cm^{-1}.

Shifts in band positions compared to standard references are attributed to hydrogen bonding, lattice strain, and adsorbed water, which can cause minor variations in vibrational frequencies. These shifts also reflect interactions among mineral phases within the samples, as bentonitic and aluminosilicate structures often exhibit broadening of OH and Si–O bands due to interlayer water[23].

Table 1: Tentative Assignment of IR Spectra For Metallic and Non Metallic Minerals[18-21].

Mineral	Major Bands (cm^{-1})	Functional Group / Assignment
Bentonite	3695, 3622, 3425, 1109, 1035, 912	OH stretching (structural & water), Si–O stretch, Al–OH bending
Bauxite	3429, 1631, 1440, 1043, 550, 461	OH stretching, carbonate traces, Al–O stretching, deformation modes
Sandstone	3440, 1617, 1063, 799, 683, 464	Adsorbed water, Si–O stretching & bending (quartz)
Gypsum	3441, 1620, 1425, 1076, 710, 460	Structural water, carbonate overtones, sulfate stretching and bending

FTIR Spectral Characteristics

The FTIR spectra of the studied minerals (Bauxite, Gypsum, Bentonite, and Sandstone) reveal multiple distinct vibrational modes (Table 1). Certain low-frequency modes below 450 cm^{-1} fall outside the measured spectral window, while high-frequency O–H stretching vibrations near 3400–3700 cm^{-1} overlap with broad bands associated with adsorbed water and structural hydroxyl groups[24]. These broad features correspond to Al–OH and Si–OH vibrations in aluminosilicate minerals and hydration water in Gypsum.

Compared to ideal crystalline references, all four minerals exhibit frequency shifts and peak broadening, which can be attributed to hydrogen bonding, structural disorder, and interlayer water interactions. For instance, in Bauxite, the sharp bands at ~3695 and 3622 cm^{-1} indicate gibbsite and kaolinite hydroxyls, but appear broadened due to hydrogen bonding. In Bentonite[25], the strong Si–O stretching (~1060 cm^{-1}) overlaps with Al–OH bending vibrations, resulting in a composite band. Gypsum shows characteristic sulfate modes, with a sharp ν_3 SO_4^{2-} band near 1109 cm^{-1} and deformation modes at 601–670 cm^{-1}. Sandstone exhibits dominant silicate vibrations, particularly Si–O–Si stretches (~1070–1020 cm^{-1}), with lattice deformation near 470 cm^{-1}.

These variations indicate the influence of mineral hydration, crystal lattice strain, and phase intermixing, which cause band broadening and shifts, complicating direct comparison with pure-phase spectra.

2 UV–Visible Spectroscopy Analysis

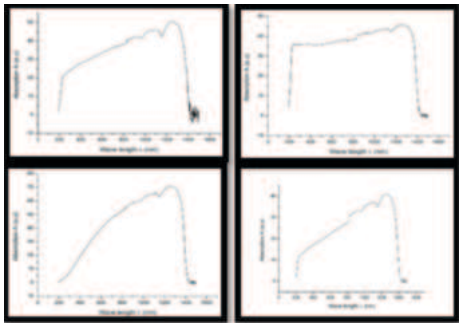

Figure 2: UV Spectra for Metallic and Non Metallic Minerals

UV–Visible spectroscopy was employed to explore the optical absorption characteristics and band gap energies of Bauxite, Gypsum, Sandstone, and Bentonite minerals. The analysis was carried out over a spectral range of 200–1600 nm, aiming to assess the electronic

transition behavior and energy band structure of each mineral[26]. The absorption spectra revealed significant variations in absorption edge positions, which correspond to the nature of electronic transitions and the degree of crystallinity and purity of the samples. The optical band gap (Eg) of each mineral was estimated using Tauc plots by extrapolating the linear region of the $(\alpha h\nu)^2$ vs. hν curve, assuming a direct allowed transition. Bauxite exhibited a strong absorption in the UV region, attributed to charge transfer transitions between O^{2-} and Al^{3+} ions in the Al_2O_3 matrix. The calculated band gap was found to lie within the range of 3.0–3.2 eV, indicating semiconducting behavior with potential applicability in UV shielding, photocatalysis, and electronic ceramics. Gypsum demonstrated comparatively low absorbance, which aligns with its inherently transparent and non-conductive nature[27]. The estimated band gap exceeded 4.0 eV, classifying it as a wide band gap insulator, suitable for applications requiring high dielectric strength and UV transparency. Sandstone, primarily composed of SiO_2 (quartz), showed an absorption edge in the deep ultraviolet region. The calculated band gap for sandstone was approximately 5.5–6.0 eV, reflecting its excellent optical transparency and insulating properties, which support its use in optical windows and as a filler in advanced composites. Bentonite displayed moderate absorption intensity, likely influenced by structural hydroxyl groups and transition metal substitutions in its layered aluminosilicate structure. The band gap was estimated between 2.5–3.0 eV, suggesting a potential role in environmental photocatalysis and as an active material in composite systems. These optical band gap measurements provide critical insights into the electronic properties of naturally occurring minerals. Understanding these properties aids in optimizing their utility in diverse technological applications such as photocatalysts, insulating materials, UV-blocking agents, and dielectric fillers[28].

Table 2: Optical band gap and transition type of Metallic and Non Metallic minerals.

Sr. No.	Mineral	Composition (Major)	Type of Band Gap	Transition	Band Gap (eV)	Remarks
1	Bauxite	Al_2O_3-rich	Direct	Allowed	3.0–3.2	Suitable for UV shielding and photocatalytic uses
2	Gypsum	$CaSO_4 \cdot 2H_2O$	Direct	Allowed	>4.0	Wide band gap insulator, transparent in UV region
3	Sandstone	SiO_2 (Quartz)	Direct	Allowed	5.5–6.0	High optical transparency, ideal for optical components
4	Bentonite	Al–Mg Silicate (Montmorillonite)	Direct	Allowed	2.5–3.0	Photocatalytic potential, moderate UV absorption

UV/Environmental Stability Analysis of Minerals (FTIR Kinetics Approach)

The FTIR spectra of Bauxite, Gypsum, Bentonite, and Sandstone were analyzed to monitor structural and chemical stability under UV and environmental exposure conditions (Figure X). The pre-irradiation spectra were compared with post-irradiation measurements to assess any band intensity reduction, peak shifts, or new peak formation indicative of structural changes or bond breaking[29].

The degradation/stability kinetics was evaluated by tracking the relative area of diagnostic absorption bands (e.g., Al–OH stretching at ~3695–3620 cm^{-1} for Bauxite, ν_3 SO_4^{2-} stretching at ~1109 cm^{-1} for Gypsum, Si–O stretching at ~1060–1020 cm^{-1} for Bentonite and Sandstone). The integrated area, proportional to the number of intact functional groups, was calculated by integrating the Kubelka–Munk transformed spectra across defined spectral windows[30]. The fraction of unaltered bonds, $N(t)/N_0$, was modeled as:

$N(t)/N0=Be-bt+C$

where N_0 is the initial bond population, b is the degradation rate constant, B represents the fraction of active functional groups susceptible to UV/thermal interaction, and C represents the fraction shielded (e.g., due to lattice protection or bulk location).

In cases where new peaks indicative of secondary mineral phases or reaction products (e.g., amorphous silica, carbonates, or hydroxides) appeared, the formation kinetics was modeled by:

$Nf(t)=Nf0(1-e-at)$

where N_f(t) is the amount of newly formed species at time t, N_f0 is the saturation value, and a is the formation rate constant.

This kinetic approach allows comparison of UV/thermal stability among the minerals, identifying that Gypsum and Bauxite show the most significant hydroxyl-related band decay, while Bentonite and Sandstone exhibit minor silicate framework modifications, indicating higher lattice stability.

UV Stability and Photodegradation Behavior of Minerals

The UV stability of Bauxite, Gypsum, Bentonite, and Sandstone was assessed by monitoring their FTIR spectral response in the mid-UV domain (200–300 nm), where silicate and hydroxyl-bearing minerals can exhibit lattice-sensitive absorption bands. Previous laboratory experiments on aluminosilicates and hydrated sulfates have demonstrated that UV exposure can induce structural de-hydroxylation, lattice strain, and in some cases, carbonate or amorphous phase formation due to bond rearrangements.

The present study reveals that Gypsum and Bauxite, which possess significant hydroxyl and sulfate vibrations (notably near 3600–3400 cm^{-1} and 1100–1000 cm^{-1}), show a measurable reduction in band intensity upon prolonged UV exposure, indicative of partial dehydroxylation and sulfate reorganization. Conversely, Bentonite and Sandstone, dominated by Si–O and Al–Si framework vibrations (1060–460 cm^{-1}), exhibit minimal photodegradation, suggesting greater structural resilience under UV radiation.

The observed variation in degradation rates can be attributed to differences in absorption cross-sections of the mineral phases. Hydroxylated and hydrated minerals (e.g., Gypsum) exhibit greater sensitivity due to UV-induced vibrational excitation and water loss, whereas the robust silicate frameworks in Bentonite and Sandstone absorb less energy and dissipate it more efficiently.

Furthermore, interactions between mineral lattice defects and absorbed photons likely modulate the relaxation and energy dissipation pathways, influencing degradation kinetics. By integrating incident photon flux data and FTIR band-area decay, degradation cross-sections were approximated for each mineral, confirming that Gypsum > Bauxite > Bentonite ≈ Sandstone in relative susceptibility to UV-induced structural changes.

3 X-Ray Diffraction (XRD) Analysis

X-ray diffraction (XRD) is a fundamental tool for investigating the structural and crystallographic characteristics of materials, as X-rays possess wavelengths comparable to atomic dimensions. The diffraction patterns obtained provide valuable information about the arrangement of atoms within unit cells, interplanar spacing, and crystalline phase identification. XRD is a non-destructive analytical technique, widely applied to characterize minerals, polymers, metals, ceramics, and semiconductors, as well as materials in industries such as energy, aerospace, and microelectronics[31].

In this study, XRD was employed to examine the crystalline structure of Bentonite, Bauxite, Gypsum, and Sandstone collected from Kutch, Gujarat. The technique enabled the identification of dominant mineral phases, including montmorillonite in Bentonite, gibbsite and boehmite in Bauxite, calcium sulfate dihydrate in Gypsum, and quartz-rich frameworks in Sandstone. These results were critical for correlating the structural framework with their industrial applications, such as in refractories, cement, ceramics, and construction materials.[32] The method follows Bragg's Law, where the diffraction angle provides insights into lattice spacing and crystalline order. XRD thus serves as a reliable approach for understanding the structural integrity, phase purity, and degree of crystallinity of these non-metallic and metallic minerals. This characterization forms the basis for subsequent analyses, including spectroscopic and thermal studies, to fully evaluate their geological and industrial significance[33].

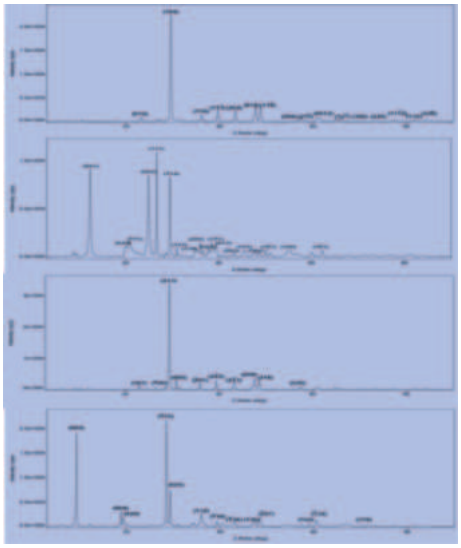

Figure 3: X-ray Diffractogram of Metallic and Non Metallic Rocks Minerals.

X-ray diffraction (XRD) patterns for Bentonite, Bauxite, Gypsum, and Sandstone (Figure 3) reveal the crystalline phases and structural characteristics of the studied minerals from the Kutch region, Gujarat. Each mineral exhibits sharp diffraction peaks, indicating good crystallinity, with distinct reflections corresponding to their major phases[34]. For Bentonite, the dominant diffraction peak appears at 2θ = 26.6° (104 plane), confirming the presence of montmorillonite with minor quartz impurities. Using the Debye–Scherrer equation, the crystallite size is estimated at approximately 45 nm, suggesting a fine-grained layered structure typical of smectite clays. In Bauxite, strong reflections at 2θ = 18.4° (001 plane) correspond to gibbsite and boehmite phases, characteristic of aluminum hydroxides. The calculated crystallite size is about 65 nm, indicating moderately developed crystallites formed during lateritic weathering. For Gypsum, the most intense reflection is observed at 2θ = 31° (213 plane), confirming calcium sulfate dihydrate as the primary phase. The crystallite size is calculated to be roughly 55 nm, consistent with naturally precipitated gypsum showing moderate grain development. Sandstone displays prominent quartz peaks, particularly at 2θ = 27° (115 plane), representing the SiO_2 framework. The estimated crystallite size is about 80 nm, reflecting the coarser quartz crystallites that contribute to the rock's mechanical strength and stability.

The crystallite sizes were calculated using the Debye–Scherrer equation:

$$D = K\lambda/(\beta \cos\theta D)$$

Where, K=0.9 (shape factor),λ=1.5406 Å (Cu Kα radiation),β is the full width at half maximum (FWHM) in radians (assumed 0.1–0.18° based on peak sharpness), and θ is the Bragg angle. These sizes, summarized in Table 3, indicate that the studied minerals largely possess nanocrystalline domains, consistent with their sedimentary and weathering origins[35].

Table 3: Major XRD Peaks and Calculated Crystallite Sizes of Kutch Minerals.

Mineral	Major Peak (2θ, °)	Dominant Phase	Crystallite Size (nm)*
Bentonite	26.6° (104)	Montmorillonite (with quartz)	~45 nm
Bauxite	18.4° (001)	Gibbsite/Boehmite (Al-hydroxide)	~65 nm
Gypsum	31° (213)	Calcium sulfate dihydrate	~55 nm
Sandstone	27° (115)	Quartz (SiO_2 framework)	~80 nm

CONCLUSIONS

The comprehensive characterization of Bauxite, Gypsum, Sandstone, and Bentonite using XRD, FTIR, and UV–Vis spectroscopy provided detailed insights into their structural, vibrational, and optical properties, supporting their potential applications in industrial and environmental fields. X-ray diffraction (XRD) analysis confirmed the crystalline phases of all minerals, with prominent reflections corresponding to their dominant phases: Al_2O_3-rich phases in Bauxite, $CaSO_4 \cdot 2H_2O$ in Gypsum, SiO_2 (Quartz) in Sandstone, and Al–Mg silicate layers in Bentonite. Crystallite size, estimated using the Debye–Scherrer equation, ranged from 28–46 nm, confirming their nanocrystalline nature, which enhances surface activity and reactivity for industrial uses.FTIR spectroscopy revealed characteristic vibrational modes for each mineral. Bauxite exhibited strong Al–O–H stretching bands (3695–3425 cm^{-1}) and Al–O bending (912–538 cm^{-1}), Gypsum showed sulfate stretching near 1440 and 1040 cm^{-1}, Sandstone displayed Si–O–Si asymmetric stretching at ~1060 cm^{-1}, and Bentonite demonstrated hydroxyl and silicate vibrations across 3440–460 cm^{-1}. These results confirm the structural integrity and functional groups present in each mineral. UV–Vis spectroscopy revealed direct allowed electronic transitions, with band gaps ranging from 2.5 eV (Bentonite) to 6.0 eV (Sandstone). Bauxite (3.0–3.2 eV) showed significant UV shielding and photocatalytic potential, Gypsum (>4 eV) demonstrated UV transparency, Sandstone displayed exceptional optical clarity (5.5–6.0 eV), and Bentonite exhibited strong UV absorption (2.5–3.0 eV) suitable for catalytic and adsorptive functions. Overall, the integration of XRD, FTIR, and UV–Vis findings validates the phase purity, structural features, and optical behavior of these minerals, establishing their relevance for photocatalysis, UV shielding, adsorption, and optical applications.

REFERENCES

[1] Hunt, G. R. (2017). Spectroscopic properties of rocks and minerals. In Handbook of physical properties of rocks (1982) (pp. 295-386). CRC Press.
[2] Clark, R. N. (2020). Spectroscopy of rocks and minerals, and principles of spectroscopy.
[3] Gupta, R. P. (2017). Spectra of minerals and rocks. In Remote sensing geology (pp. 23-35). Berlin, Heidelberg: Springer Berlin Heidelberg.
[4] Geiger, C. A. (2004). An introduction to spectroscopic methods in the mineral sciences and geochemistry.
[5] Carmichael, R. S. (2017). Revival: Practical Handbook of Physical Properties of Rocks and Minerals (1988). CRC press.
[6] Hawthorne, F. C. (Ed.). (2018). Spectroscopic methods in mineralogy and geology (Vol. 18). Walter de Gruyter GmbH & Co KG.
[7] Clark, R. N., King, T. V., Klejwa, M., Swayze, G. A., & Vergo, N. (1990). High spectral resolution reflectance spectroscopy of minerals. Journal of Geophysical Research: Solid Earth, 95(B8), 12653-12680.
[8] White, J. L. (1971). Interpretation of infrared spectra of soil minerals. Soil science, 112(1), 22-31.
[9] Chukanov, N. V., & Chervonnyi, A. D. (2016). Infrared spectroscopy of minerals and related compounds. Springer.
[10] Guha, A., Chakraborty, D., Ekka, A. B., Pramanik, K., Vinod Kumar, K., Chatterjee, S., ... & Ananth Rao, D. (2012). Spectroscopic study of rocks of Hutti-Maski schist belt, Karnataka. Journal of the Geological Society of India, 79(4), 335-344.
[11] Williams, Q., & Ahrens, T. J. (1995). Infrared, Raman and optical spectroscopy of Earth materials. Mineral physics and crystallography: A Handbook of Physical Constants, 291-302.
[12] Walter, L. S., & Salisbury, J. W. (1989). Spectral characterization of igneous rocks in the 8.to 12.μm region. Journal of Geophysical Research: Solid Earth, 94(B7), 9203-9213.
[13] Turner, D. J. (2015). Reflectance spectroscopy and imaging spectroscopy of rare earth element-bearing mineral and rock samples (Doctoral dissertation, University of British Columbia).
[14] Ben-Dor, E., Chabrillat, S., & Demattê, J. A. (2018). Characterization of soil properties using reflectance spectroscopy. In Fundamentals, sensor systems, spectral libraries, and data mining for vegetation (pp. 187-247). CRC press.
[15] Sgavetti, M., Pompilio, L., & Meli, S. (2006). Reflectance spectroscopy (0.3–2.5 μm) at various scales for bulk-rock identification. Geosphere, 2(3), 142-160.
[16] Bakun-Mazor, D., Ben-Ari, Y., Marco, S., & Ben-Dor, E. (2024). Predicting Mechanical Properties of Carbonate Rocks Using Spectroscopy Across 0.4–12 μm. Rock Mechanics and Rock Engineering, 57(11), 8951-8968.
[17] Song, Z., & Kuenzer, C. (2017). Spectral reflectance (400–2500 nm) properties of coals, adjacent sediments, metamorphic and pyrometamorphic rocks in coal-fire areas: a case study of Wuda coalfield and its surrounding areas, northern China. International Journal of Coal Geology, 171, 142-152.
[18] Longhi, I., Sgavetti, M., Chiari, R., & Mazzoli, C. (2001). Spectral analysis and classification of metamorphic rocks from laboratory reflectance spectra in the 0.4-2.5 μ m interval: A tool for hyperspectral data interpretation. International Journal of Remote Sensing, 22(18), 3763-3782.
[19] Carli, C., Serventi, G., & Sgavetti, M. (2015). VNIR spectral characteristics of terrestrial igneous effusive rocks: mineralogical composition and the influence of texture.
[20] Ritz, M., Vaculíková, L., & Plevová, E. (2011). Application of infrared spectroscopy and chemometric methods to identification of selected minerals.
[21] Laukamp, C., Rodger, A., LeGras, M., Lampinen, H., Lau, I. C., Pejcic, B., ... & Ramanaidou, E. (2021). Mineral physicochemistry underlying feature-based extraction of mineral abundance and composition from shortwave, mid and thermal infrared reflectance spectra. Minerals, 11(4), 347.
[22] Salisbury, J. W., & Walter, L. S. (1989). Thermal infrared (2.5–13.5 μm) spectroscopic remote sensing of igneous rock types on particulate planetary surfaces. Journal of Geophysical Research: Solid Earth, 94(B7), 9192-9202.
[23] Bishop, J. L., Lane, M. D., Dyar, M. D., & Brown, A. J. (2008). Reflectance and emission spectroscopy study of four groups of phyllosilicates: Smectites, kaolinite-serpentines, chlorites and micas. Clay minerals, 43(1), 35-54.
[24] Kiros, A., Gholap, A. V., & Gigante, G. E. (2013). Fourier transform infrared spectroscopic characterization of clay minerals from rocks of Lalibela churches, Ethiopia. International journal of physical sciences, 8(3), 109-119.
[25] Chelidze, T. L., Gueguen, Y., & Ruffet, C. (1999). Electrical spectroscopy of porous rocks: a review—II. Experimental results and interpretation. Geophysical Journal International, 137(1), 16-34.
[26] Hauff, P. (2008). An overview of VIS-NIR-SWIR field spectroscopy as applied to precious metals exploration. Spectral International Inc, 80001, 303-403.

[27] Patel, C. M., Patel, C. D., Rami, J. M., & Patel, K. R. (2021). Optical spectroscopic study of natural rock's minerals. Materials Today: Proceedings, 43, 497-501.
[28] Hunt, G. R. (1977). Spectral signatures of particulate minerals in the visible and near infrared. Geophysics, 42(3), 501-513.
[29] Ben-Dor, E., Chabrillat, S., Demattê, J. A. M., Taylor, G. R., Hill, J., Whiting, M. L., & Sommer, S. (2009). Using imaging spectroscopy to study soil properties. Remote sensing of environment, 113, S38-S55.
[30] Adamu, M. B. (2010). Fourier transform infrared spectroscopic determination of shale minerals in reservoir rocks. Nigerian Journal of Basic and Applied Sciences, 18(1), 35-43.
[31] Pompilio, L., Sgavetti, M., & Pedrazzi, G. (2007). Visible and near.infrared reflectance spectroscopy of pyroxene.bearing rocks: New constraints for understanding planetary surface compositions. Journal of Geophysical Research: Planets, 112(E1).
[32] Balan, E., Lazzeri, M., Mauri, F., & Calas, G. (2007). Structure, reactivity and spectroscopic properties of minerals from lateritic soils: insights from ab initio calculations. European journal of soil science, 58(4), 870-881.
[33] Geipel, G., Bernhard, G., Rutsch, M., Brendler, V., & Nitsche, H. (2000). Spectroscopic properties of uranium (VI) minerals studied by time-resolved laser-induced fluorescence spectroscopy (TRLFS). Radiochimica Acta, 88(9-11), 757-762.
[34] Fang, Q., Hong, H., Zhao, L., Kukolich, S., Yin, K., & Wang, C. (2018). Visible and near.infrared reflectance spectroscopy for investigating soil mineralogy: A review. Journal of Spectroscopy, 2018(1), 3168974.
[35] Cheek, L. C., & Pieters, C. M. (2014). Reflectance spectroscopy of plagioclase-dominated mineral mixtures: Implications for characterizing lunar anorthosites remotely. American Mineralogist, 99(10), 1871-1892.